

Quasi periodic oscillations in active galactic nuclei

William Alston^{1,*}, Andy Fabian¹, Julija Markevičiūtė², Michael Parker¹,
Matt Middleton¹, and Erin Kara¹

¹ Institute of Astronomy, Madingley Rd, Cambridge, CB3 0HA, UK

² Department of Applied Mathematics and Theoretical Physics, Centre for Mathematical Sciences, Wilberforce Rd, Cambridge CB3 0WA

Received 3 September 2015

Key words galaxies: active - accretion, accretion disks - black hole physics - galaxies: individual RE J1034+396 - galaxies: individual MS 2254.9–3712

Quasi-periodic oscillations (QPOs) are coherent peaks of variability power observed in the X-ray power spectra (PSDs) of stellar mass X-ray binaries (XRBs). A scale invariance of the accretion process implies they should be present in the active galactic nuclei. The first robust detection was a ~ 1 hr periodicity in the Seyfert galaxy RE J1034+396 from a ~ 90 ks *XMM-Newton* observation, however, subsequent observations failed to detect the QPO in the $0.3 - 10.0$ keV band. In this talk we present the recent detection of the ~ 1 hr periodicity in the $1.0 - 4.0$ keV band of 4 further low-flux/spectrally-harder observations of RE J1034+396 (see Alston et al 2014). We also present recent work on the discovery of a QPO in the Seyfert galaxy, MS 2254.9–3712, which again is only detected in energy bands associated with the primary power-law continuum emission (Alston et al 2015). We conclude these features are most likely analogous to the high-frequency QPOs observed in XRBs. In both sources, we also see evidence for X-ray reverberation at the QPO frequency, where soft X-ray bands and Iron $K\alpha$ emission lag the primary X-ray continuum. These time delays may provide another diagnostic for understanding the underlying QPO mechanism observed in accreting black holes.

© 0000 WILEY-VCH Verlag GmbH & Co. KGaA, Weinheim

1 Introduction

One of the most important breakthroughs in the study of stellar mass black holes was the discovery of high frequency quasi-periodic oscillations (HFQPOs; with $\nu_{\text{QPO}} \gtrsim 40$ Hz) in Galactic black hole X-ray binaries (XRBs), with $M_{\text{BH}} \sim 10 M_{\odot}$ (Morgan, Remillard & Greiner 1997; Remillard et al 1999; Strohmayer et al 2001; Remillard et al 2002, 2003; van der klis 2006; Remillard & McClintock 2006). Sixteen years of RXTE observations have yielded detections in a handful of sources (see Belloni, Sanna & Mendez 2012; Altamirano & Belloni 2012; Belloni & Altamirano 2013a,b, and references therein).

These are the fastest coherent variability signatures observed from XRBs, with frequencies close to Keplerian frequency of the innermost stable circular orbit (ISCO). HFQPOs are therefore expected to carry information on the strongly curved spacetime close to the black hole, providing constraints on the two fundamental properties of black holes: mass and spin.

Despite their importance, the exact mechanism responsible for producing HFQPOs remains one of the biggest challenges in contemporary astrophysics, with varying scenarios for the origin of the oscillation presented in the literature (e.g. Milsom & Taam 1997; Nowak et al 1997; Wagoner 1999; Stella et al 1999; Abramowicz & Kluzniak 2001;

Rezzolla et al 2003; Das & Czerny 2011, see also Motta, S., this volume).

If strong gravity dominates the accretion process, a scale invariance implies that HFQPOs should also be present in Active Galactic Nuclei (AGN; $M_{\text{BH}} \gtrsim 10^6 M_{\odot}$). With a black hole (BH) mass ratio $M_{\text{BHB}}/M_{\text{AGN}} = 10^{-5}$ we expect $\nu_{\text{QPO}} \gtrsim 5 \times 10^{-3}$ Hz (i.e. timescales of $\gtrsim 200$ s) in AGN, well within the temporal passband of e.g. *XMM-Newton*. AGN have higher counts per characteristic timescale, allowing us to potentially study individual QPO periods, providing a better opportunity to understand this phenomenon.

QPOs are notoriously difficult to detect in AGN, primarily due to insufficient observation lengths currently available with *XMM-Newton* (Vaughan & Uttley 2005, 2006). Many reported detections have been disfavoured due to inaccuracy of modelling the underlying red noise continuum (Vaughan 2005; Vaughan & Uttley 2005, 2006; Gonzalez-Martin & Vaughan 2012). A ~ 1 hr periodicity in the Seyfert galaxy RE J1034+396 was the first robust detection of a QPO in an AGN (Geirllinski et al 2008, see also Vaughan 2010).

Accreting BHs also display *hard* lags at low frequencies — where variations in harder energy bands are delayed with respect to softer energy bands (e.g. Alston et al 2014 and references therein). The leading model for the origin of the hard lags is the radial propagation of random accretion rate fluctuations through a stratified corona (e.g. Arevalo & Uttley 2006 and references therein).

* Corresponding author: e-mail: wna@ast.cam.ac.uk

Soft X-ray lags at higher frequencies has now been observed in $\gtrsim 20$ AGN (e.g. Fabian et al 2009; Emmanoulopoulos et al 2011; Zoghbi 2011; Alston et al 2013; Cackett et al 2013; De Marco et al 2013; Kara et al 2013; Alston et al 2014). A picture is emerging where the *reverberation* signal is produced when the primary X-ray emission is reprocessed by the inner accretion disc (see Uttley et al 2014 for a review). High frequency iron $K\alpha$ lags have also been observed, adding more weight to the inner reverberation scenario (e.g. Zoghbi et al 2012; Zoghbi et al 2013; Kara et al 2013). See talks by Cackett, E., De Marco, B., Ingram, A., Kara, E., Uttley, P. in this volume for more on time delays in accreting sources.

The time lags of HFQPOs in XRBs have also been studied, with Mendez et al (2013) recently carrying out a systematic study in 4 sources. They found both hard and soft lags are observed at the QPO and harmonic frequencies. The interpretation of these HFQPO time lags is still unclear, however, they provide an extra diagnostic for understanding their physical origin.

In this talk, I will present recent work on HFQPOs in two AGN: RE J1034+396 and MS 2254.9–3712, as well as their associated variability properties.

2 Recent QPO detections in AGN

2.1 RE J1034+396

RE J1034+396 is a nearby ($z = 0.042$) NLS1 galaxy with $M_{\text{BH}} \sim 2 \times 10^6 M_{\odot}$ and thought to be accreting at or above the Eddington rate ($L/L_{\text{Edd}} \sim 1$; e.g. Jin et al 2012). This led Middleton & Done (2010) and Middleton et al (2011, hereafter M10 and M11, respectively) to conclude that the QPO in RE J1034+396 is an analogue of the 67 Hz QPO in the super-Eddington BHB GRS 1915+105. Four further *XMM-Newton* observations of RE J1034+396 were analysed in M11 in an attempt to confirm the QPO in this source. Restricting the PSD analysis to the 0.3 – 10.0 keV band revealed no sign of the QPO at any frequency, leading M11 to conclude the QPO was a transient feature. However, similarities between the covariance spectra (Wilkinson & Uttley 2009) were seen between the original 90 ks observation and two other observations. Further attempts at understanding the QPO in RE J1034+396 have so far been limited to the one 90 ks observation (Czerny et al 2010; M10; Czerny et al 2012; Hu et al 2014).

2.1.1 Power-spectrum analysis

In this work we present an energy resolved PSD analysis of RE J1034+396, see Alston et al 2014b (hereafter, A14) for full details. We used all eight archival *XMM-Newton* observations, spanning 2002 to 2011. Light curves were extracted following standard methods in a soft (0.3–1.0 keV) and hard (1.0–4.0 keV) bands (see Figure 1 in A14). The hard band was chosen to provide a high S/N light curve of the primary continuum. PSDs were estimated by calculating the

periodogram (e.g. Priestley 1981; Percival & Walden 1993; Vaughan et al 2003a). We fitted the PSDs using the maximum likelihood method described in Vaughan 2010, see A14 for fit details.

We used two simple continuum models that are commonly used to fit AGN PSDs (e.g. Uttley et al 2002; Vaughan & Fabian 2003; Vaughan et al 2003a,b; McHardy et al 2004; Gonzalez-Martin Vaughan 2012). Model 1 is the simplest model consisting of a power law plus constant:

$$P(\nu) = N\nu^{-\alpha} + C \quad (1)$$

where N is the normalisation term and C is a non-negative constant used to model the Poisson noise level. Model 2 is a bending power-law (e.g. McHardy et al 2004):

$$P(\nu) = \frac{N\nu^{\alpha_{\text{low}}}}{1 + (\nu/\nu_{\text{bend}})^{\alpha_{\text{low}} - \alpha_{\text{high}}}} + C \quad (2)$$

where ν_{bend} is the bend frequency, α_{low} and α_{high} are power-law slopes below and above ν_{bend} respectively. In Model 2 we fixed $\alpha_{\text{low}} = 1$, which is the typical value found from long-term X-ray monitoring studies (e.g. Uttley et al 2002; Markowitz et al 2003; McHardy et al 2004; Gonzalez-Martin Vaughan 2012). A variant of this model (Model 3) with $\alpha_{\text{low}} = 0$ is used as the significance of QPO features has a strong dependence on the continuum modelling (e.g. Vaughan & Uttley 2005, 2006). The model fits to the 4 low-flux/spectrally harder observations are shown in Fig. 1.

Using a likelihood ratio test we find that the simple model 1 is preferred all the time for all energy bands. A significant outlier (i.e low p -value) is found in the hard band (1.0–4.0 keV) in the five observations which have a lower flux and are spectrally harder, including the original 90 ks observation. No significant outliers are observed in the soft or total bands in these 5 observations, with the exception of the 90 ks observation. No significant outliers are observed at any energy in the two higher flux / spectrally softer observations. The fractional variability amplitude of the feature is $\sim 5\%$ in each of the 5 observations. A quality factor $Q = \nu/\Delta\nu \gtrsim 10$ is observed in the 5 detections.

2.2 MS 2254.9–3712

MS 2254.9–3712 is a nearby ($z = 0.039$; Stocke 1991) ‘unabsorbed’ ($N_{\text{H}} < 2 \times 10^{22} \text{ cm}^{-2}$; Grupe et al 2004) narrow line Seyfert 1 (NLS1) galaxy, with X-ray luminosity $\log(L_{\text{X}}) = 43.29 \text{ erg s}^{-1}$. The central BH mass in MS 2254.9–3712 is estimated as $M_{\text{BH}} \sim 4 \times 10^6$ using the empirical $R_{\text{BLR}} - \lambda L_{\lambda}(5100\text{\AA})$ relation (Grupe et al 2004; Grupe et al 2010) and is estimated as $M_{\text{BH}} \sim 10^7$ using the $M_{\text{BH}} - \sigma$ relation (Shields et al 2003). The Eddington rate is estimated as $L_{\text{Bol}}/L_{\text{Edd}} = 0.24$ using $\lambda L_{\lambda}(5100\text{\AA})$ (Grupe et al 2004; Grupe et al 2010). However, Wang et al 2003 suggest MS 2254.9–3712 is accreting at super-Eddington rate ($\dot{M}/\dot{m}_{\text{Edd}} > 1$).

We model the PSD in MS 2254.9–3712 in a similar manner to RE J1034+396 (see Alston et al 2015, hereafter

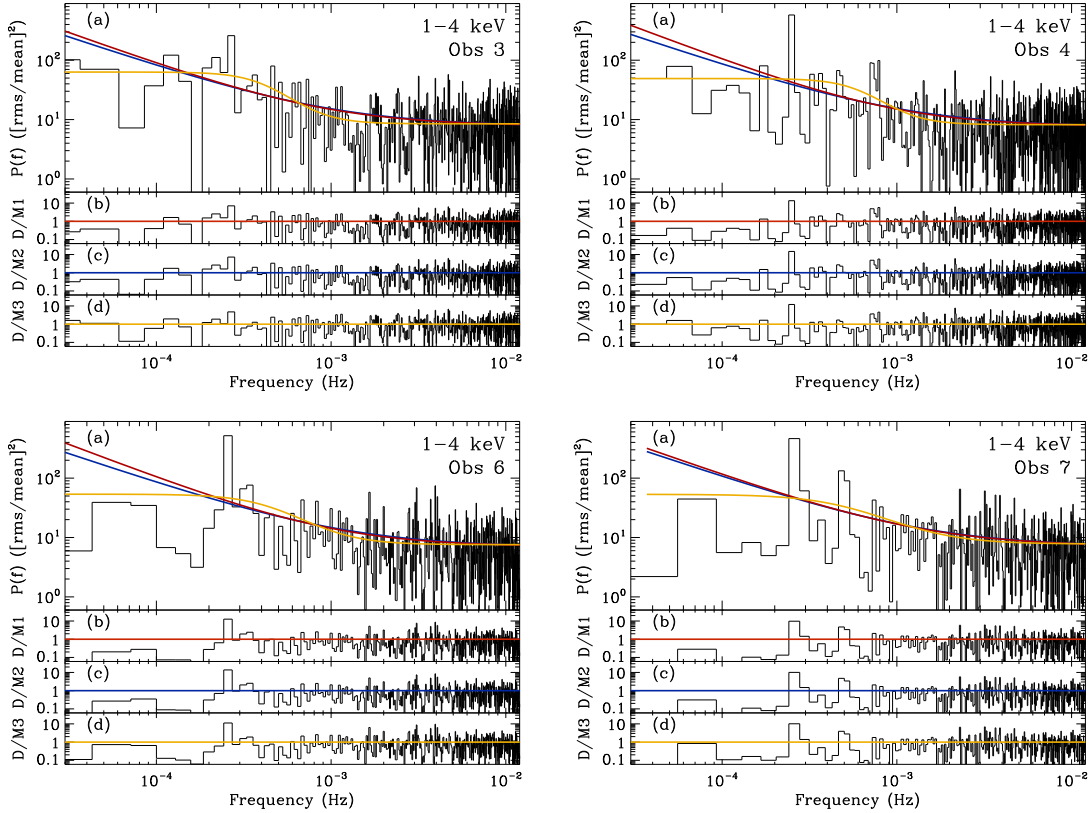


Fig. 1 The model fits to the 1.0 – 4.0 keV PSDs of Obs3,4,6 and 7 in RE J1034+396 (see A14 for observation details). In panel (a) is the data and PSD model fits for Model 1 (red), Model 2 (blue) and Model 3 (yellow). Panels (b), (c) and (d) show the data/model residuals for models 1, 2 and 3 respectively. The frequency of the QPO has remained the same over 5 years of observations. A tentative harmonic component is seen in Obs 7. Figures reproduced from A14.

A15). Fig. 2 shows the model fits to the 1.2 – 5.0 keV band, where a significant outlier can be seen at $\sim 1.5 \times 10^{-4}$ Hz (~ 2 hrs). No significant features are observed in other energy bands. The fractional variability amplitude of the feature is $\sim 6\%$ and the quality factor $Q = 8$, consistent to what is observed in RE J1034+396.

3 Frequency resolved time delays

In this section we explore the frequency-dependent time delays between different energy bands in both RE J1034+396 and MS 2254.9–3712. This allows us to study any reprocessed emission that is responding to the QPO modulation.

Following Vaughan & Nowak (1997) we calculate the cross-spectrum in M non-overlapping time series segments, then average over the M estimates at each Fourier frequency. Cross-spectra were averaged over adjacent frequency bins geometrically by a factor 1.15 in frequency. From the complex valued cross-spectrum we obtain a phase lag estimate at each frequency, $\phi(f)$, which gives the corresponding time lag $\tau(f) = \phi(f)/(2\pi f)$. Errors are estimated following e.g. Bendat & Piersol (1986); Vaughan & Nowak (1997).

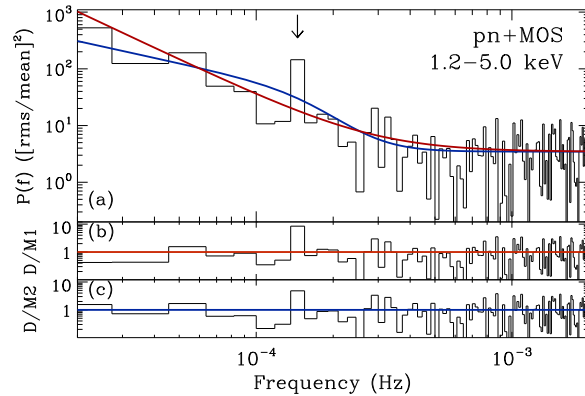


Fig. 2 The 1.2–5.0 keV band PSD and model fits are shown in panel (a), for model 1 (red) and model 2 (blue). The data/model residuals for models 1 and 2 are shown in panels (b) and (c), respectively. Figure reproduced from A15.

For RE J1034+396 we make use of only the 5 observations where the QPO is detected (A14; Markeviciute et al, *in prep*). Fig. 3 (top panel) shows the frequency dependent time lags between the 0.3 – 0.8 keV and 1.0 – 4.0 keV bands. A positive lags indicates the hard band is lagging. At

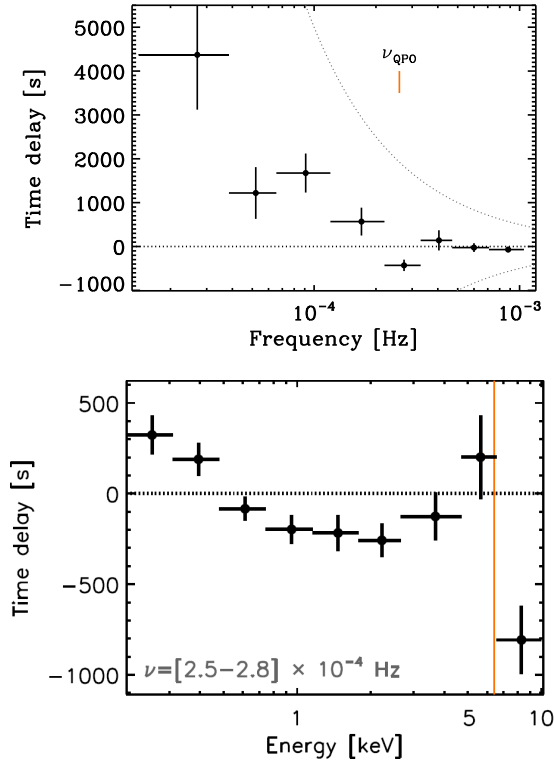


Fig. 3 Time delays in RE J1034+396. The top panel shows the time delay as a function of Fourier frequency between the hard (1.0 – 4.0 keV) and soft (0.3 – 0.8 keV) bands. Positive values indicate a hard band lag. A hard lag is observed at low frequencies, which switches to a soft (negative) lag at the QPO frequency ($\sim 2.6 \times 10^{-4}$ Hz). The bottom panel shows the lag-energy spectrum on the QPO frequency. A soft lag is observed as well as a lag in the iron $K\alpha$ band. Figures to appear in Markeviciute et al *in prep*.

low frequencies a hard lag is observed, whereas at the QPO frequency, a negative (soft) lag is observed (see also Zoghbi et al 2011).

A related technique is the *lag-energy* spectrum: time delays at a given frequency as a function of energy. The lag-energy spectrum is calculated by estimating the time delay between a comparison energy band vs a broad (in energy) reference band (e.g. Zoghbi 2011; Alston et al 2014a; Uttley et al 2014). When the comparison energy band falls within the reference band that light curve is subtracted from the reference band, in order to avoid correlated errors. Fig. 3 (bottom panel) shows the lag-energy spectrum for RE J1034+396 on the QPO timescale, where a positive lag indicates a given energy band lags the reference band (Markeviciute et al *in prep*). The whole 0.3 – 10.0 keV band is used as the reference band. A ~ 500 s soft lag can be seen as well as a lag ~ 1000 s at energy bands around the 6.4 keV iron $K\alpha$ feature.

Fig. 4 (top panel) shows the frequency dependent time lags between the 0.3 – 0.7 keV and 1.2 – 5.0 keV bands in MS 2254.9–3712 (see Alston et al 2015 for more details).

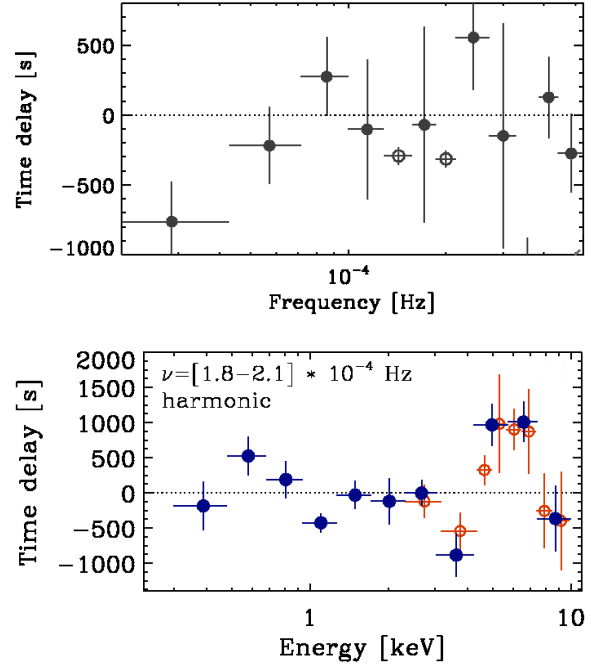


Fig. 4 Time delays in MS 2254.9–3712. The top panel shows the time delay as a function of Fourier frequency between the hard (1.2 – 5.0 keV) and soft (0.3 – 0.7 keV) bands. A soft (negative) lag is observed at the QPO frequency ($\sim 1.5 \times 10^{-4}$ Hz) and harmonic frequency ($\sim 2 \times 10^{-4}$ Hz). The bottom panel shows the lag-energy spectrum on the harmonic frequency, where a lag in the iron $K\alpha$ band is observed. Figures reproduced from A15.

A significant soft lag is seen at the QPO frequency, and at a frequency in an approximately 3:2 ratio with the QPO (open symbols). No significant hard lag is observed in MS 2254.9–3712 on the timescales we can probe, but a $\sim 3\sigma$ soft lag is observed at the lowest frequency.

The lag energy-spectrum for the QPO frequency in MS 2254.9–3712 shows a soft lag, but no lag at iron $K\alpha$ (see Fig. 6 in A15). The lag-energy spectrum for the harmonic frequency is shown in Fig. 4 (bottom panel). The 0.3 – 5.0 keV band is used as the reference. A lag of ~ 1000 s is observed between the continuum dominated bands and the $\sim 5 - 7$ keV band, which contains the iron $K\alpha$ band.

4 Conclusions

4.1 Summary

We have presented recent work on QPOs in two AGN: RE J1034+396 and MS 2254.9–3712, including investigation of their time delays. The results are summarised as follows:

- Using the Bayesian posterior predictive method of Vaughan (2012) we assess various continuum models to the observed data. We then test for the presence of any interesting additional features where a low p -value

is taken as evidence for an additional feature. Significant narrow outliers are considered as evidence for the presence of a QPO.

- The QPO at $\sim 2.6 \times 10^{-4}$ Hz (~ 1 hrs) in RE J1034+396 has been detected in four new *XMM-Newton* observations, spanning ~ 5 years. The feature is only detected in the hard band (1.0 – 4.0 keV) in observations that are lower in flux and are spectrally harder. This increases the observation time where a QPO is detected in this source to ~ 250 ks. There is tentative evidence for a harmonic component in one observation (Obs 7).
- A new QPO at $\sim 1.5 \times 10^{-4}$ Hz (~ 2 hrs) is detected in the NLS1 galaxy, MS 2254.9–3712. Again, the feature is only detected in the continuum dominated band, 1.2 – 5.0 keV.
- The fractional variability of the features are 5 and 6 percent and quality factor, $Q \gtrsim 10$ and 8 in RE J1034+396 and MS 2254.9–3712, respectively.
- The two sources share many of the same variability properties, including rms-spectra and principle components analysis (see A14 and A15 for more details).
- Investigation of the time delays between energy bands as a function of Fourier frequency reveals soft lags at the QPO frequency (and harmonic frequency in MS 2254.9–3712). Iron K α like lags are seen at the QPO frequency in RE J1034+396, but only the harmonic frequency in MS 2254.9–3712.

4.2 Discussion

The central black hole mass of RE J1034+396 is uncertain, with best estimates are putting it at $\sim 1 - 4 \times 10^6 M_{\odot}$ (e.g. Bian & Huang 2010; Jin et al 2011). Based on this mass estimate and the inferred $L/L_{\text{Edd}} \gtrsim 1$, M10 and M11 proposed the QPO in RE J1034+396 was analogous with the 67 mHz QPO in GRS 1915+105. However, Mendez et al 2013 observed a soft-lag in the 35 mHz HFQPO in GRS 1915+105 (Belloni & Altamirano 2013). A soft lag is observed at the QPO frequency (see also Zoghbi et al 2011), leading Mendez et al 2013 to suggest the QPO in RE J1034+396 is an analogue of the 35 mHz QPO in GRS 1915+105. The potential harmonic feature we see in Obs7 of RE J1034+396 (Fig. 1) could then be the analogue of the 67 mHz QPO in GRS 1915+105.

The mass of the BH in MS 2254.9–3712 is highly uncertain, with no reverberation mapping mass measurement for this source. In A15 we argue that the QPO is more consistent with the HFQPO type seen in XRBs. HFQPOs in XRBs have a typical fractional rms ~ 5 per cent (Remillard & McClintock 2006), consistent with the 6 per cent value observed here. A $Q \gtrsim 2$ is observed in HFQPOs in XRBs (e.g. Casella et al 2004), again consistent with our value of $Q \sim 8$. HFQPOs in XRBs often display harmonic components, with an integer ratio of 3:2 (e.g. Remillard et al 2002,

2003; Remillard & McClintock 2006). Strong evidence for the presence of a 3:2 harmonic component is observed in MS 2254.9–3712, suggesting this is a HFQPO.

The origin of HFQPOs is still highly uncertain, but it is clear that the physical mechanism occurring in the direct vicinity of the BH. If indeed we are seeing iron K α reverberation responding to the QPO process, this will allow us to understand both the QPO mechanism in better detail, and provide important constraints for any model for the HFQPO mechanism. Whether these are the same kind of lagging mechanism that is seen in other Seyferts (e.g. Uttley et al 2014) remains an open question.

Acknowledgements. WNA, ACF and EK acknowledge support from the European Union Seventh Framework Programme (FP7/2013–2017) under grant agreement n.312789, StrongGravity. This paper is based on observations obtained with *XMM-Newton*, an ESA science mission with instruments and contributions directly funded by ESA Member States and the USA (NASA).

References

- Abramowicz, M. A., & Kluźniak, W. 2001, *A&A*, 374, L19
 Alston, W. N., Vaughan, S., & Uttley, P. 2013, *MNRAS*, 435, 1511
 Alston, W. N., Done, C., & Vaughan, S. 2014a, *MNRAS*, 439, 1548
 Alston, W. N., Markevičiūtė, J., Kara, E., Fabian, A. C., & Middleton, M. 2014b, *MNRAS*, 445, L16 (A14)
 Alston, W. N., Parker, M. L., Markevičiūtė, J., et al. 2015, *MNRAS*, 449, 467 (A15)
 Alston, W. N., et al. *in prep*
 Markevičiūtė, J., Alston, W. N., et al. *in prep*
 Altamirano, D., & Belloni, T. 2012, *ApJ*, 747, L4
 Arévalo, P., & Uttley, P. 2006, *MNRAS*, 367, 801
 Belloni, T. M., Sanna, A., & Méndez, M. 2012, *MNRAS*, 426, 1701
 Belloni, T. M., & Altamirano, D. 2013a, *MNRAS*, 432, 19
 Belloni, T. M., & Altamirano, D. 2013b, *MNRAS*, 432, 10
 Bian, W.-H., & Huang, K. 2010, *MNRAS*, 401, 507
 Cackett, E. M., Fabian, A. C., Zoghbi, A., et al. 2013, *ApJ*, 764, L9
 Casella, P., Belloni, T., Homan, J., & Stella, L. 2004, *A&A*, 426, 587
 Czerny, B., Lachowicz, P., Dovčiak, M., et al. 2010, *A&A*, 524, A26
 Czerny, B., Lachowicz, P., Dovčiak, M., et al. 2012, *Journal of Physics Conference Series*, 372, 012055
 Das, T. K., & Czerny, B. 2011, *MNRAS*, 414, 627
 De Marco, B., Ponti, G., Cappi, M., et al. 2013, *MNRAS*, 431, 2441
 Emmanoulopoulos, D., McHardy, I. M., & Papadakis, I. E. 2011, *MNRAS*, 416, L94
 Fabian, A. C., Zoghbi, A., Ross, R. R., et al. 2009, *Nature*, 459, 540
 Gierliński, M., Middleton, M., Ward, M., & Done, C. 2008, *Nature*, 455, 369
 González-Martín, O., & Vaughan, S. 2012, *A&A*, 544, A80
 Grupe, D., Wills, B. J., Leighly, K. M., & Meusinger, H. 2004, *AJ*, 127, 156
 Grupe, D., Komossa, S., Leighly, K. M., & Page, K. L. 2010, *ApJS*, 187, 64

- Hu, C.-P., Chou, Y., Yang, T.-C., & Su, Y.-H. 2014, *ApJ*, 788, 31
- Jin, C., Ward, M., Done, C., & Gelbord, J. 2012, *MNRAS*, 420, 1825
- Kara, E., Fabian, A. C., Cackett, E. M., et al. 2013, *MNRAS*, 428, 2795
- Kara, E., Fabian, A. C., Cackett, E. M., et al. 2013, *MNRAS*, 434, 1129
- Kara, E., Zoghbi, A., Marinucci, A., et al. 2015, *MNRAS*, 446, 737
- Markevičiūtė, J., Alston, W. N., et al. *in prep*
- Markowitz, A., Edelson, R., Vaughan, S., et al. 2003, *ApJ*, 593, 96
- McHardy, I. M., Papadakis, I. E., Uttley, P., Page, M. J., & Mason, K. O. 2004, *MNRAS*, 348, 783
- Méndez, M., Altamirano, D., Belloni, T., & Sanna, A. 2013, *MNRAS*, 435, 2132
- Middleton, M., & Done, C. 2010, *MNRAS*, 403, 9 (M10)
- Middleton, M., Done, C., Ward, M., Gierliński, M., & Schurch, N. 2009, *MNRAS*, 394, 250
- Middleton, M., Uttley, P., & Done, C. 2011, *MNRAS*, 417, 250 (M11)
- Parker, M. L., Marinucci, A., Brenneman, L., et al. 2014, *MNRAS*, 437, 721
- Parker, M. L., Fabian, A. C., Matt, G., et al. 2015, *MNRAS*, 447, 72
- Remillard, R. A., & McClintock, J. E. 2006, *Ann. Rev. A&A*, 44, 49
- Rezzolla, L., Yoshida, S., Maccarone, T. J., & Zanotti, O. 2003, *MNRAS*, 344, L37
- Shields, G. A., Gebhardt, K., Salvander, S., et al. 2003, *ApJ*, 583, 124
- Stella, L., Vietri, M., & Morsink, S. M. 1999, *ApJ*, 524, L63
- Strohmayer, T. E. 2001, *ApJ*, 552, L49
- Uttley, P., McHardy, I. M., & Papadakis, I. E. 2002, *MNRAS*, 332, 231
- Uttley, P., Cackett, E. M., Fabian, A. C., Kara, E., & Wilkins, D. R. 2014, *A&ARv*, 22, 72
- Vaughan, S., & Fabian, A. C. 2003, *MNRAS*, 341, 496
- Vaughan, S., Edelson, R., Warwick, R. S., & Uttley, P. 2003, *MNRAS*, 345, 1271
- Vaughan, S., Fabian, A. C., & Nandra, K. 2003, *MNRAS*, 339, 1237
- Vaughan, S. 2005, *A&A*, 431, 391
- Vaughan, S., & Uttley, P. 2005, *MNRAS*, 362, 235
- Vaughan, S., & Uttley, P. 2006, *Advances in Space Research*, 38, 1405
- Vaughan, S. 2010, *MNRAS*, 402, 307
- Vaughan, S., Uttley, P., Pounds, K. A., Nandra, K., & Strohmayer, T. E. 2011, *MNRAS*, 413, 2489
- Wagoner, R. V. 1999, *Phys. Rep.*, 311, 259
- Wilkinson, T., & Uttley, P. 2009, *MNRAS*, 397, 666
- Zoghbi, A., & Fabian, A. C. 2011, *MNRAS*, 418, 2642
- Zoghbi, A., Fabian, A. C., Reynolds, C. S., & Cackett, E. M. 2012, *MNRAS*, 422, 129
- Zoghbi, A., Cackett, E. M., Reynolds, C., et al. 2014, *ApJ*, 789, 56